Overview of the TRIPOLI-4 Monte Carlo code, version 12

François-Xavier Hugot, Alexis Jinaphanh, Cédric Jouanne, Coline Larmier, Yi Kang Lee, Davide Mancusi, Odile Petit, Thierry Visonneau, Andrea Zoia

EPJ Nuclear Sci. Technol. **10**, 17 (2024)

https://doi.org/10.1051/epjn/2024018

EPJ Nuclear Sciences & Technologies

Available online at:
https://www.epj-n.org

Status and advances of Monte Carlo codes for particle transport simulation, edited by Andrea Zoia, Cheikh Diop and Cyrille de Saint Jean

REGULAR ARTICLE

OPEN ACCESS

Overview of the TRIPOLI-4 Monte Carlo code, version 12

François-Xavier Hugot, Alexis Jinaphanh, Cédric Jouanne, Coline Larmier, Yi Kang Lee, Davide Mancusi, Odile Petit, Thierry Visonneau and Andrea Zoia*

Université Paris-Saclay, CEA, Service d'Etudes des Réacteurs et de Mathématiques Appliquées, 91191 Gif-sur-Yvette, France

Received: 10 June 2024 / Received in final form: 27 August 2024 / Accepted: 3 October 2024

Abstract. In this paper we present an overview of the recent advances of the general-purpose Monte Carlo code TRIPOLI-4®, developed at CEA. The features described in this work, which refer to the current version 12 of the code, encompass applications to radiation shielding (variance-reduction methods: Consistent Adjoint-Driven Importance Sampling, Adaptive Multilevel Splitting, and Weight Windows), material activation calculations (Rigorous Two-Step Scheme), reactor physics (fission matrix, kinetics parameters, critical parameter search, kinetics with delayed neutron precursors), criticality-safety (perturbation and sensitivity methods: Standard and Generalized Perturbation Theory) and nuclear instrumentation (fission models, improvements in the electromagnetic shower models, and coupling with the code Geant4).

1 Introduction

TRIPOLI-4® is the general-purpose particle-transport Monte Carlo code developed at CEA, with the support of EDF, for applications encompassing radiation shielding, material activation, criticality-safety, reactor physics including fuel depletion, and nuclear instrumentation [1]. The development of the fourth generation of TRIPOLI-4 started at the beginning of the 1990s [2], and the current version 12 of this generation, released in 2022, is soon to be distributed by the OECD/NEA Data Bank. A general overview of TRIPOLI-4 was provided in reference [1], in the framework of a special session on Monte Carlo codes organized for the Supercomputing in Nuclear Applications and Monte Carlo conference (SNA + MC 2013), and will be briefly recalled here, for the sake of completeness. For a thorough description, the reader is referred to reference [1]. Recent updates and publications can be found in the TRIPOLI-4 website: `https://www.cea.fr/energies/tripoli-4`.

TRIPOLI-4 is a continuous-energy particle-transport Monte Carlo code that can simulate neutrons, photons (including photo-nuclear reactions), and electrons/positrons (coupled to photons within the electromagnetic shower models). Nuclear data are read directly from the ENDF format [3], without any pre-processing through ACE files[1]; probability tables for the unresolved resonance range are generated by the CALENDF code [4], developed at CEA. The Doppler Broadening Rejection Correction method allows resonance elastic scattering cross-sections to be taken into account [5].

Several geometry engines are available, encompassing the native combinatorial and surface-based geometries (or any combinations thereof), and those using the ROOT package [6]. The code can be run in a single-processor or parallel mode; for this latter, it relies on a proprietary, built-in, communication library using BSD sockets [7] or on the MPI standard.

The simulation modes of TRIPOLI-4 encompass both fixed-source propagation [8] and k-eigenvalue calculations [9]. For fuel depletion and material activation problems, TRIPOLI-4 relies on the Bateman equations solver MENDEL [10], developed at CEA.

The code has several standard tallies, including particle flux, reaction rates, currents, deposited energy, radiation damage effects (gas production and DPAs), and dose equivalent rates. Perturbations in fixed-source and eigenvalue calculations can be computed using the correlated sampling [11] or the Taylor expansion [12] methods; furthermore, TRIPOLI-4 can tally the Green's function relating a given source to the detector [13], which is useful to quickly compute the effects of different sources to the tallies. A built-in module, called INIPOND [14], is capable of automatically generating an approximate importance function to be fed to the exponential transform method, the legacy strategy of TRIPOLI-4 for importance-driven variance reduction in radiation shielding applications [15].

* e-mail: andrea.zoia@cea.fr

[1] Note however that some of the nuclear data are rewritten in specific formats used for sampling: equi-probable cosines for the representation of angular anisotropy and Doppler-broadened interaction cross-sections are stored in the portable binary XDR format. Furthermore, photon production cross-sections for individual neutron interactions are used as such, without any summation.

Several pre and post-processing tools are available to help in the preparation of the input deck and the analysis of the output files, among which the T4G interactive graphical visualizer [16,17], relying upon the same geometry engine as TRIPOLI-4; the Valjean[2] framework for the automation of typical test suites [18], including checkout and compilation of the source code, execution of calculations, parsing of simulation results, statistical tests and generation of test reports; and the t4_geom_convert[3] MCNP→TRIPOLI geometry converter [19,20], capable of handling most of the idiomatic MCNP constructs, such as universes, lattices, macro-bodies and affine coordinate transformations (it also converts isotopic compositions and boundary conditions). Furthermore, scripts are provided to the users in order to facilitate the handling of the output file and the normalization of the obtained tallies, especially for fuel depletion.

Industrial needs and research projects have fostered many new developments since the publication of reference [1], and the community of TRIPOLI-4's users is steadily growing. Prompted by the organization of a special session on Monte Carlo codes for the SNA + MC 2024 international conference, which also coincides with the 30th anniversary of the code, in this work, we illustrate the main improvements of TRIPOLI-4 over the last decade. The development of TRIPOLI-5®, the next-generation Monte Carlo code jointly developed by CEA and IRSN with the support of EDF, will be described in a companion paper [21]. This paper is organized as follows: in Section 2 we will address applications related to reactor physics and criticality safety; in Section 3 we will consider applications related to radiation shielding and activation; and in Section 4 we will examine applications related to nuclear instrumentation. Miscellaneous improvements concerning the geometry will be described in Section 5. Conclusions will be finally drawn in Section 6.

2 Reactor physics and criticality-safety applications

We begin our description by considering the novel features of TRIPOLI-4 devoted to reactor physics and criticality-safety applications.

2.1 Simulation modes

In addition to the standard fission-generation-based power iteration to determine the fundamental k-eigenvalue and the associated fundamental eigenmode of the k-eigenvalue formulation of the Boltzmann equation, TRIPOLI-4 has been endowed with new simulation modes. To begin with, two history-based methods have been implemented [22,23]: the Wielandt method, based on an eigenvalue-shift approach leading to an average (user-defined) number of inner generations within outer generations [24], and the super-history method, whereupon each outer generation is decomposed in a (user-defined) fixed number of inner generations [25].

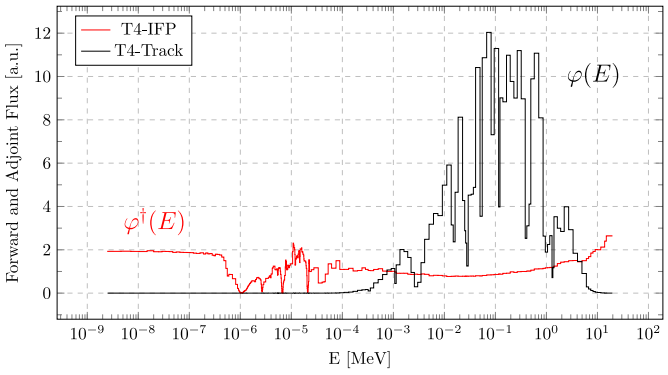

Fig. 1. Comparison between forward $\varphi(E)$ and adjoint $\varphi^\dagger(E)$ fundamental eigenmodes, for a MOX fuel pin-cell. The forward flux (black) is computed using the track estimator within the standard power iteration; the adjoint flux (red) is computed using the IFP method. Figure taken from reference [27]. (This figure is subject to copyright protection and is not covered by Creatice Commons License. Elsevier, 2018).

The history-based approaches are known to help in quenching the correlations in (forward) k-eigenvalue calculations [24,25]; they are also key to enabling a useful trade-off between memory burden and computation time for calculations involving adjoint-weighted tallies, such as sensitivity coefficients [26], and this was an additional motivation for the implementation of these methods in TRIPOLI-4, as illustrated in Section 2.5.

Furthermore, TRIPOLI-4 can now compute the fundamental joint k-eigenmode, based on a modified fixed-source calculation where neutron histories are simulated over a user-defined amount of fission generations using a super-history algorithm. The neutron progeny attaining the last generation is used to infer the importance of the ancestor neutron (emitted from the source), and this tally allows thus estimating the scalar product of the source with the adjoint eigenmode [27]. For illustration, Figure 1 shows the forward and adjoint eigenmodes of a MOX fuel pin-cell computed with TRIPOLI-4.

2.2 Fission matrix

TRIPOLI-4 can compute the fission matrix ($K_{i,j}$[4]) over the cells of the Monte Carlo model or a user-defined mesh [29], which allows for performing spectral analysis and assessing in particular the dominance ratio. The $K_{i,j}$ capabilities of TRIPOLI-4 have been further extended: the code can re-use the stored matrix to initialize the fission sources of the power iteration based on an estimate of the fundamental k-eigenmode, which allows reducing the number of inactive fission cycles needed to achieve convergence. An investigation of the convergence pattern of power iteration with and without $K_{i,j}$-based on initialization of the fission sources has been extensively carried out. A recent application to the EOLE critical facility of

[2] https://valjean.readthedocs.io/en/v0.11.0-alpha.0/index.html

[3] https://github.com/arekfu/t4_geom_convert

[4] The normalized contribution of a neutron born in a cell j in a given generation to fission events in the cell i at the following generation [28].

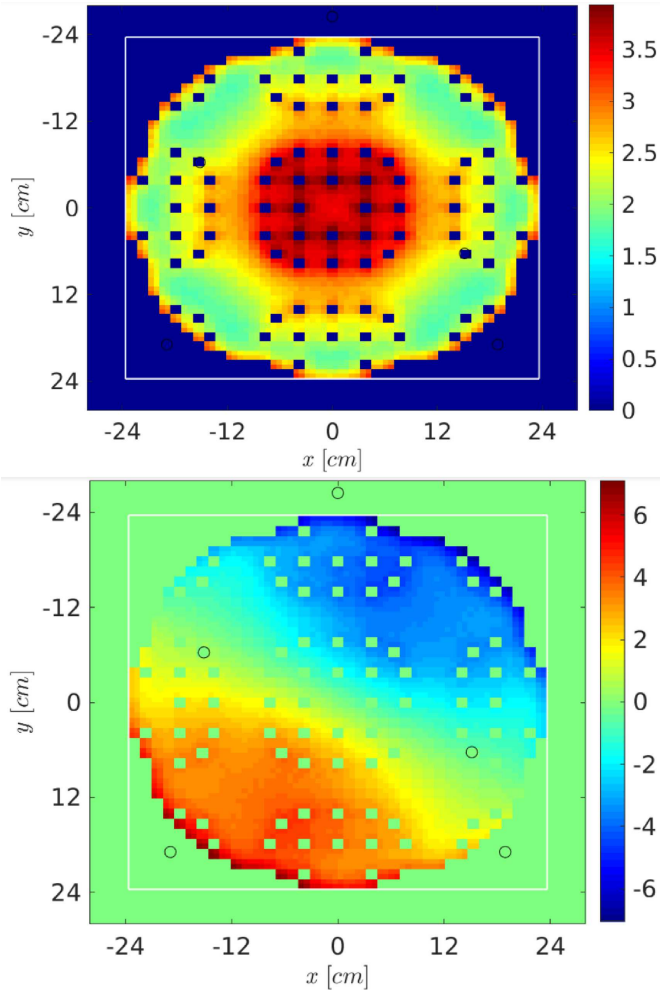

Fig. 2. Radial cut of the fundamental (top) and first excited eigenmode (bottom) of the fission source distribution of the EOLE critical facility, formerly operated by CEA. The eigenmodes have been computed using the fission matrix ($K_{i,j}$) capability of TRIPOLI-4. Figure adapted from reference [30]. (This figure is subject to copyright protection and is not covered by Creatice Commons License. Elsevier, 2021).

CEA is discussed, e.g., in reference [30], and is illustrated in Figure 2.

2.3 Critical parameter search

The key advantage of Monte Carlo simulation over deterministic solvers is the almost complete absence of discretization errors and the use of all available information contained in nuclear data libraries. Yet, Monte Carlo models of real-world systems are typically affected by a 'bias' concerning measured values, because of uncertainties in technological specifications and/or the quality of nuclear data libraries. For some reactor physics applications, such as determining the fundamental eigenmode to be fed as an initial state to a time-dependent simulation (see e.g. Sect. 2.6), it is important to ensure that the Monte Carlo model is critical when the corresponding real-world system is also critical. In TRIPOLI-4, this condition can be established in several ways.

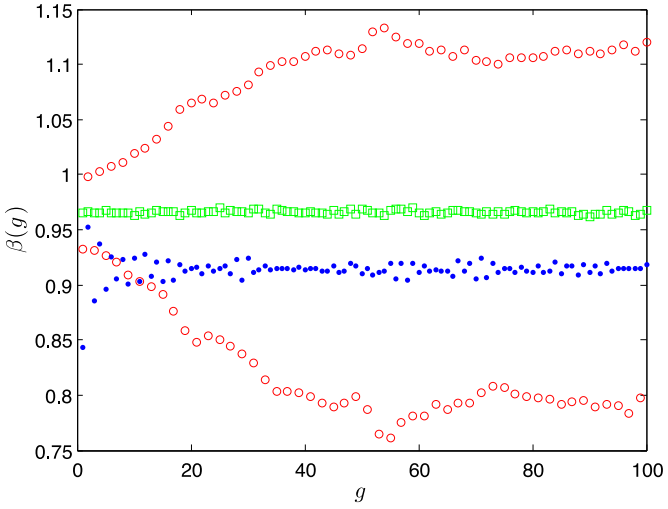

Fig. 3. Critical albedo search applied to a UOX fuel assembly: evolution of the surface albedo $\beta(g)$ as a function of the number of fission cycles g. Blue: beginning-of-life conditions (slightly super-critical); red: higher burn-up (slightly sub-critical): the critical parameter search would fail, unless the speed of convergence is adjusted (green), in which case the algorithm converges to the sought value. Figure taken from reference [31]. (This figure is subject to copyright protection and is not covered by Creatice Commons License. Elsevier, 2018).

The simplest approach consists in normalizing the total fission multiplicity by the fundamental k eigenvalue of the system, determined in a separate calculation. Alternatively, TRIPOLI-4 allows performing a critical parameter search, i.e., determining the critical value of a control parameter that makes the system critical: for this purpose, the code relies on the standard power iteration and iteratively adjusts a free parameter of the model based on the value of the fundamental k eigenvalue, in order for k to attain a unit value at the end of the search procedure. Currently, the critical parameter search can be applied to the boron content in one or several material compositions of the model, and to the albedo value on one or several surface boundary conditions of the model [31].

Special care has been taken in order to prevent the critical parameter search from falling into numerical instabilities due to the non-linear nature of the coupling between the power iteration and the parameter adjustment. Stabilization techniques based on eigenvalue shift or changes in the speed of convergence are available [31]. For illustration, a critical albedo search applied to a UOX fuel assembly is displayed in Figure 3.

2.4 Kinetics parameters and reactor constants

TRIPOLI-4 is endowed with several methods to estimate kinetics parameters, which are key quantities for reactor safety [34]. The first approach relies on fission-weighting, which yields the natural reactor constants: the delayed

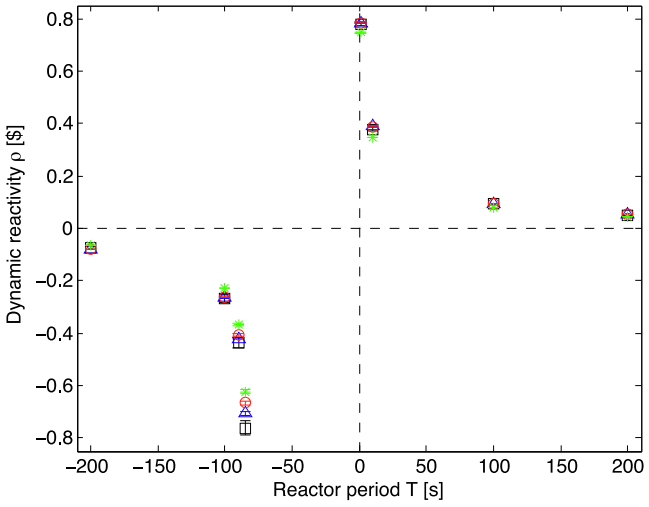

Fig. 4. Reference and computed dynamic reactivity of the IPEN/MB-01 core. Benchmark values (black) are compared to TRIPOLI-4 calculations using JEFF-3.1.1 (blue), ENDF/B-VII.r0 (green), and JENDL-4.0 (red) nuclear data. Figure taken from reference [37]. (This figure is subject to copyright protection and is not covered by Creatice Commons License. Elsevier, 2017).

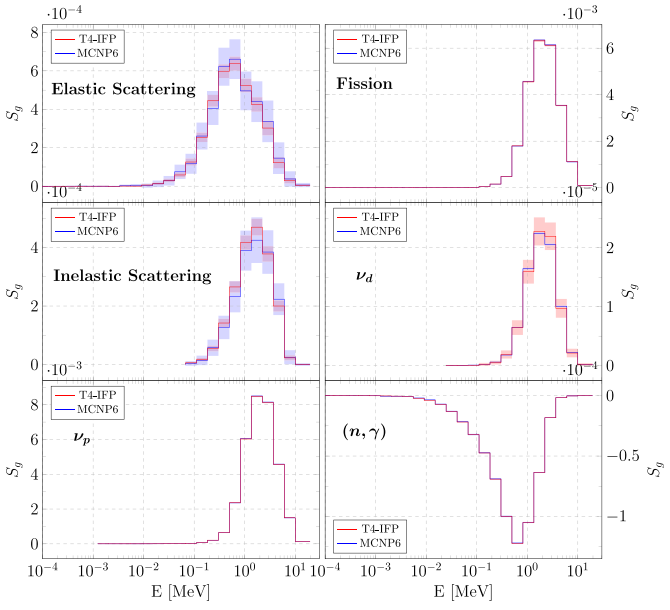

Fig. 5. Sensitivity profiles (decomposed over a 33-group mesh) of the k-eigenvalue concerning sections and fission multiplicities of ^{240}Pu for the JEZEBEL benchmark. Comparison between TRIPOLI-4 and MCNP6 using the JEFF-3.1.1 nuclear data library. Shaded areas correspond to one-sigma statistical uncertainties. Figure taken from reference [38]. (This figure is subject to copyright protection and is not covered by Creatice Commons License. Elsevier, 2018).

neutron fraction β (total and decomposed for each precursor family), the average neutron lifetime Λ (total or conditioned to particular events: mean generation time, mean absorption time and mean leakage time), the precursor decay constants λ_j for each family j, and the average β_j-weighted decay constant $\bar{\lambda}$. The delayed neutron fractions can be further decomposed for each fissile nuclide.

The second approach relies on the Iterated Fission Probability (IFP) method [32,33], which allows estimating adjoint-weighted tallies and yields the effective kinetics parameters as commonly defined in terms of ratios of bi-linear forms, weighted by both the adjoint and forward fundamental eigen-modes: the effective delayed neutron fraction β_{eff} (total and decomposed for each precursor family), the effective neutron mean generation time Λ_{eff}, and the Rossi alpha parameter $\alpha_{\text{Rossi}} = -\beta_{\text{eff}}/\Lambda_{\text{eff}}$. Again, the delayed neutron fraction can be further decomposed for each fissile nuclide. The number of latent generations needed for the IFP to reach the asymptotic value is a user-defined parameter, and TRIPOLI-4 monitors the convergence during the simulation. The IFP algorithm implemented in the code uses overlapping latent generations, which reduces the required computation time [34]. Since the number of kinetics parameters to be estimated in a single calculation is rather small, IFP is particularly convenient: the memory burden is relatively modest, and the simulation time overhead is small. Optionally, the effective kinetics parameters can be also estimated using history-based methods (either Wielandt or super-history). The calculation of kinetics parameters has been extensively validated based on international benchmarks and data from experimental facilities [34–37]. For illustration, the dynamic reactivity of the IPEN/MB-01 reactor benchmark inferred based on kinetics parameters estimated using the IFP method is displayed in Figure 4.

In addition to the kinetics parameters, TRIPOLI-4 can compute several other reactor constants of interest. The migration area is estimated using the mean squared displacement between birth from fission and death from absorption or leakage. Similarly, as for kinetics parameters, the migration area can be unweighted, or adjoint-weighted. The parameters occurring in the six-factor formula (fast fission and (n, xn) reaction effects, resonance escape probability, thermal utilization factor, thermal reproduction factor, and leakage probability, which generalize Fermi's standard four-factor formula) are estimated based on reaction rates decomposed over two energy groups, the boundary between groups being a free parameter. The slowing down current across a given energy yields a spectral index for the characterization of the reactor behavior. Finally, the Diven factor, accounting for the dispersion of the fission multiplicity, is also estimated using user-provided data or a fission model (see Sect. 4.4).

2.5 Perturbations and sensitivities

TRIPOLI-4 relies on the general framework of the Standard Perturbation Theory (SPT) to compute first-order reactivity perturbations [38] and k-eigenvalue sensitivity coefficients to nuclear data [38,39], and on the Generalized Perturbation Theory (GPT) to compute the sensitivity of reaction rate ratios and kinetics parameters to nuclear data [40–42]. For this purpose, the adjoint fundamental eigenmode is estimated by resorting either to the IFP

method [43,44] or to history-based methods (Wielandt or super-history [45]), over a user-defined number of latent generations. Similarly, as for effective kinetics parameters, the choice between IFP or history-based methods relies on a trade-off between memory occupation and computation time [42]: in this case, however, the typical number of perturbations or sensitivity coefficients that are to be estimated within a single simulation can be very large, so that history-based methods (which reduce the memory burden at the expense of an increased computation time) should be favored.

Reactivity coefficients can be computed concerning variations in the nuclide concentrations, in the material densities, in the cross sections (over a given energy interval), and in the average fission multiplicity (prompt or delayed, total or per precursor family, each over a given energy interval) [38]. The coefficients can be further decomposed into the fission, scattering, and collision components, and the first-order formula can be improved by adjusting the denominator as proposed in reference [43].

Sensitivity coefficients of the k-eigenvalue to nuclear data parameters (SPT) can be computed with respect to cross sections, average fission multiplicity, fission spectra (prompt or delayed, total or per precursor family) and scattering laws [38]. Each coefficient is decomposed over a given incident energy mesh; fission spectra coefficients are decomposed over the incident and outgoing energies, and those of scattering laws are decomposed with respect to the incident energy and the scattering cosine mesh. The standard SPT estimators do not take into account the normalization of the sensitivity to fission spectra and scattering laws, and lead to the so-called unconstrained sensitivity coefficients. TRIPOLI-4 can enforce the normalization constraint, which leads to the so-called constrained sensitivity coefficients, relying on a method proposed in reference [43]. The SPT capabilities have been extensively validated by comparison with respect to other Monte Carlo codes using the same or different algorithms, and have been further compared to those obtained from deterministic codes [38,39]. For illustration, the k-eigenvalue sensitivity profiles for the JEZEBEL benchmark are displayed in Figure 5.

Sensitivity coefficients of reaction rate ratios to nuclear data parameters (GPT) can be computed with respect to cross sections, average fission multiplicity, fission spectra (prompt or delayed, total or per precursor family), and scattering laws [40]. For this purpose, the user assigns a nuclide, a reaction rate, and one (or several) cell(s) or material composition(s), separately for the numerator and for the denominator of the ratio. Contrary to the reactivity coefficients and the SPT, for which both IFP and history-based implementations are available in TRIPOLI-4, the implementation of the GPT relies exclusively on the super-history method, combined with the Differential Operator Sampling approach [45]. The GPT capabilities [40–42] have also been extensively validated against other codes and methods. For illustration, the sensitivity profile of the fission reaction rate ratio for the UAM TMI pin-cell benchmark is shown in Figure 6.

In the development version of TRIPOLI-4, GPT routines have been extended to the sensitivity of kinetics parameters (encompassing the effective delayed neutron fraction, the effective mean generation time, and the effective mean lifetime) to nuclear data [42]. These capabilities, which have been recently successfully validated, will be made available to users in the next release of the code.

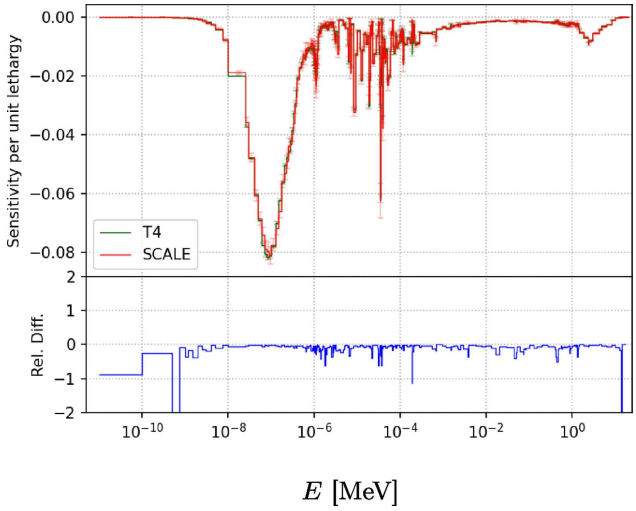

Fig. 6. Sensitivity profile of the F28/F25 reaction rate ratio (fission cross section) on ^{235}U for the UAM TMI pin-cell benchmark. Comparison between TRIPOLI-4 and SCALE results. Figure taken from reference [42]. (This figure is subject to copyright protection and is not covered by Creatice Commons License. Taylor & Francis, 2024).

2.6 Reactor kinetics

The kinetic simulation mode of TRIPOLI-4 allows for solving the time-dependent Boltzmann equation, coupled to the M precursor equations[5], one for each delayed neutron precursor family [46]. In order to tally the sought physical observables in kinetic simulations, TRIPOLI-4 adopts a scoring time mesh: the ensemble-averaged content of each bin yields an estimate of the corresponding observable integrated between the two-time bounds of the bin. For the simulation of scenarios where reactor components (e.g., control rods) are moved, TRIPOLI-4 allows modifying the model geometry and the associated material compositions at each time step. For illustration, the simulation of a reactivity insertion and withdrawal scenario in the SPERT III E-core model is shown in Figure 7. Kinetic simulations are strongly affected by the presence of spatial clustering phenomena [47] induced by the correlations between fission events; furthermore, neutron and precursor time scales, and their respective population sizes, are typically highly unbalanced [48,49], which might lead to severe issues due to undersampling. In order to cope with these problems, TRIPOLI-4 is endowed with several variance-reduction and population-control methods that allow for achieving statistical convergence in acceptable computer time. Here we present a brief overview of the current implementation; for a thorough description, we refer the reader to references [46,50].

[5] The number of available families depends on the nuclear data libraries.

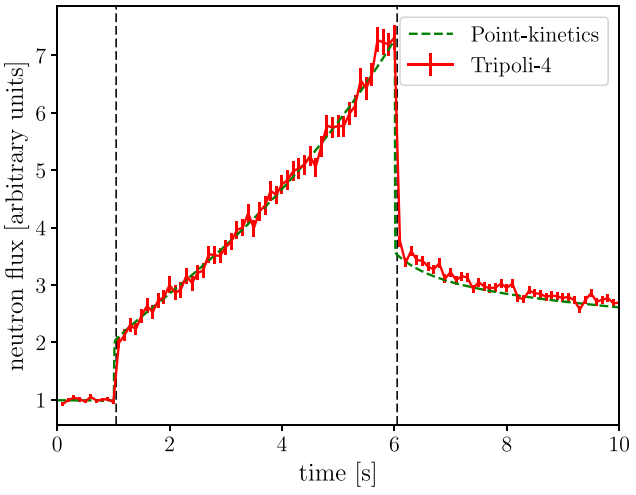

Fig. 7. Kinetic simulation of the SPERT III E-core: time evolution of the neutron flux starting from a critical state. Control rods are withdrawn at $t = 1\,\mathrm{s}$, and inserted back at $t = 6\,\mathrm{s}$. The results of the TRIPOLI-4 simulation (red) are compared to the solution of the point kinetics equations (green). Figure taken from reference [46]. (This figure is subject to copyright protection and is not covered by Creatice Commons Elsevier, 2018).

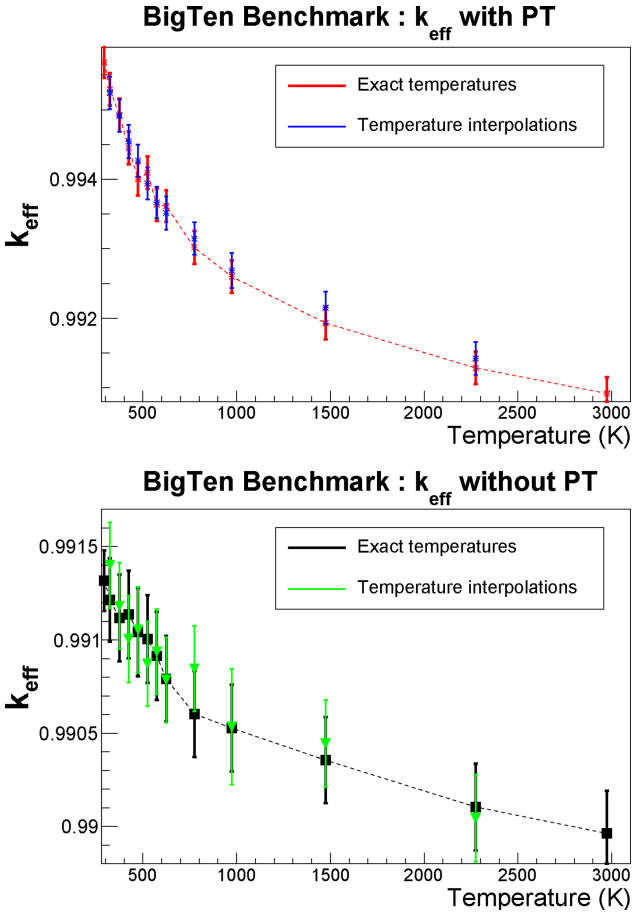

Fig. 8. Comparison of the multiplication factors k_{eff} obtained for the BigTen benchmark configuration, using (linear) stochastic interpolation or exact cross sections at a given temperature. Top: with probability tables (PT); bottom: without probability tables (PT). Dashed lines are drawn through the results using exact cross-sections, to guide the eye. Figure adapted from reference [55] (SNA+MC, 2020).

Precursors are combined into a single representative particle carrying the total statistical weight, which reduces the variance due to the dispersion of the decay constants [51]; this method preserves the unbiasedness of the average scores. Furthermore, the sampling of the precursor decay does not obey the natural exponential law, but is forced to be uniform in each bin of an arbitrary time mesh: this yields more neutrons in the fission chains, thus reducing the variance of the total population per unit time [51].

Fission events lead to branches in the neutron histories that are ultimately responsible for increased variance and spatial correlations. In order to quench the correlations induced by fission chains, TRIPOLI-4 uses the *branchless* collision method [51], which samples a single outgoing particle carrying the average weight of all the possible descendants. A weight correction ensures that branchless games are unbiased. Branchless transport is quite effective in reducing the variance in multiplying systems [50,52]. Further research work is in progress concerning the possibility of achieving highly efficient importance-sampling schemes for kinetics simulations [54] and will be implemented in future releases of TRIPOLI-4.

In the course of a kinetic simulation, the number of neutrons and precursors may rise or fall exponentially fast: both cases demand some control mechanisms in order to keep the population within reasonable bounds. For the sake of simplicity, in TRIPOLI-4 population control is enforced at the end of the time intervals used for forced decay, which has the main advantage of not introducing further stopping times for the precursors. Two population-control strategies are currently implemented: combing, and Russian roulette & splitting [51]. The latter can be separately applied to the neutron and precursor buffers at the end of each time step. For precursors, the roulette is applied based on the expected delayed neutron weight produced during the following time step. Combing normalizes the number of transported particles while preserving their total weight (and the proportion of respective weights for neutrons and precursors) [53], which allows for reducing the computational cost by ensuring that the population sizes remain roughly constant over time steps.

If the initial configuration of a kinetic simulation corresponds to the equilibrium state of a given multiplying system, TRIPOLI-4 uses the power iteration over a large number of inactive cycles, with neutrons alone, in order to obtain an estimate of the fundamental mode [46]. During the last inactive cycle, neutrons and precursors for the subsequent time-dependent simulation are sampled at each collision. In order to reduce the overhead due to the number of inactive cycles of the power iteration (which should be in principle re-run for each independent replica of the kinetic simulation), TRIPOLI-4 allows injecting the fission neutrons generated in the last inactive cycle of the current batch in the inactive cycles of the following

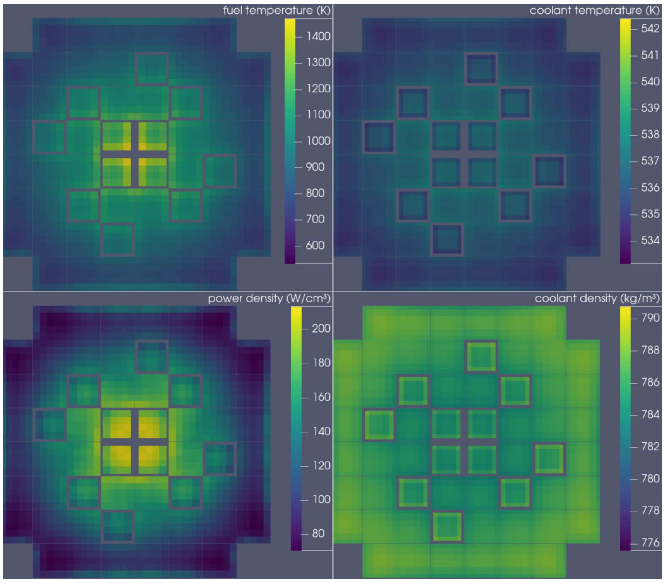

Fig. 9. Radial cuts of the fields computed by TRIPOLI-4 coupled with SubChanFlow, for the stationary state of the SPERT III E-core at 20 MW. Top left: fuel temperature; top right: coolant temperature; bottom left: power density; bottom right: coolant density. Figure taken from reference [60]. (This figure is subject to copyright protection and is not covered by Creatice Commons License. Springer Nature, 2022).

one, after skipping a few extra cycles: this procedure, however, comes at the cost of introducing correlations among the replicas.

2.7 Stochastic temperature interpolation

For reactor physics applications, one often needs to take into account material compositions having a large number of different temperatures. In view of this consideration, a stochastic temperature interpolation scheme has been developed in TRIPOLI-4 [55]. During the simulation, neutron cross-sections are generated on the fly and become available for particle flight and collision sampling without any supplementary data storage. The interpolation applies to both neutron cross-sections from evaluated data and probability tables generated from CALENDF [4]; when thermal scattering law $S(\alpha, \beta)$ data are available, interpolation is applied to the resulting cross-sections (and not directly to $S(\alpha, \beta)$, coherently with the NJOY code specifications [56]. Two different interpolation modes are available: linear and square root. For illustration, Figure 8 shows an application of this feature for criticality calculations based on the BigTen benchmark at several temperatures, with or without probability tables [55].

2.8 Multi-physics simulations

In the development version of TRIPOLI-4, an interface devoted to multi-physics applications has been conceived, allowing data transfers between the Monte Carlo code and external solvers for stationary as well as time-dependent simulations. In particular, extensive validation tests have been carried out in the context of the European H2020 project McSAFE (2017–2020) [57–60]. For illustration, the simulation of the steady state of the SPERT III E-core at 20 MW [60], involving the thermal-hydraulics feedback provided by the SubChanFlow code [61], is displayed in Figure 9. While the implementation and the tests were successful, in view of the complexity of efficiently handling the parallel execution and the memory burden involved by the multi-physics interface within the existing framework of TRIPOLI-4, further work on these topics is deferred to the development of TRIPOLI-5, which natively takes into account these issues.

3 Radiation shielding and activation applications

In this section, we discuss new features related to applications in radiation shielding and material activation.

3.1 CADIS

The Consistent Adjoint-Driven Importance Sampling (CADIS) method is a variance-reduction strategy based on feeding as an importance map for a Monte Carlo radiation-transport simulation of the solution of the adjoint Boltzmann equation discretized over a space/energy mesh by a deterministic solver [62,63]. The CADIS method, which is now widely considered one of the most successful sampling strategies for radiation shielding applications [64], has been implemented in TRIPOLI-4 [65,66] relying on IDT, a multi-group, SN deterministic solver based on the method of short characteristics [67].

In the IDT solver, spatial mesh cells are assumed to be homogeneous. In practice, a mesh cell can overlap with more than one volume of the TRIPOLI-4 model, with possibly different material compositions. IDT will assume that cells are filled with the material composition that is found at the center of the cell. This admittedly crude approximation will be improved upon in future versions of the code. The order of the SN angular quadrature to be used by IDT is set by the users: larger values of this parameter improve the accuracy of the angular quadrature formulas and help with mitigating ray effects in the importance map; however, the memory footprint and the CPU time of IDT increase for increasing values of the SN order.

IDT produces both neutron and photon importance maps; the development of the coupled neutron-photon adjoint solver is under way and will be provided in a future version of the code. For illustration, the neutron and photon importance maps for a radiation shielding application are shown in Figure 10. In the current implementation of the CADIS scheme, the importance map produced by IDT is automatically fed to the exponential transform, which is the legacy importance-sampling method of TRIPOLI-4, without any external file-processing manipulation required for the users to transfer data from the

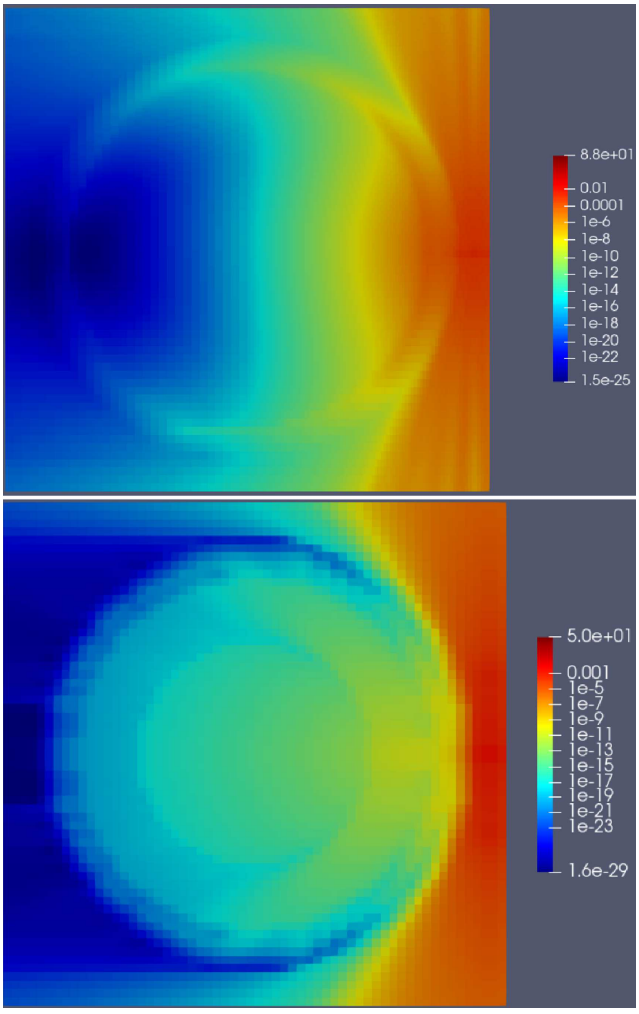

Fig. 10. Neutron (top) and photon (bottom) spatial importance maps for a radiation shielding application: computing the reaction rate at a detector located in an out-of-vessel position. The detector position corresponds to the peak of the importance maps. The maps have been computed using the IDT solver to obtain the solutions of the adjoint neutron and photon problems on a spatial and energy mesh.

deterministic solver to the Monte Carlo code. Furthermore, the importance maps generated by IDT can be exported for use with other variance-reduction methods (see Sects. 3.2 and 3.3).

The IDT solver is distributed with TRIPOLI-4; in addition, microscopic multi-group cross sections (in HDF format) are also distributed, for the sake of convenience: photon cross sections use a 94-group energy mesh, while the neutron cross sections use a 281-group energy mesh. The implementation of the CADIS method has been extensively validated by comparison with other variance-reduction methods of TRIPOLI-4 and with other Monte Carlo codes using the same or different variance-reduction methods, based on international benchmarks and reference configurations (including cases where fissile media are also present, like in reactor start-up problems with ex-core detectors) [66,68,69].

3.2 Weight windows

In TRIPOLI-4 we have also implemented the weight windows method, a variance-reduction strategy based on importance-driven splitting and Russian roulette that is currently used by several other Monte Carlo transport codes, such as MCNP [70]. This technique has shown great potential for solving radiation shielding problems, especially when the importance function required for the generation of the weight windows is obtained from the solution of the adjoint Boltzmann equation [71,72].

In the version of the weight windows technique developed in TRIPOLI-4, each weight window is defined by a lower weight bound (for the Russian roulette game, played by particles whose statistical weight is below the threshold), a survival weight (outgoing weight of particles surviving the Russian roulette game), and an upper weight (for splitting, played by particles whose statistical weight is above the threshold). No action is taken for particles whose weights lie within the window. Weight windows can be applied to neutrons and photons; for both, weight windows are enforced at collisions and optionally at surface crossings.

The current version of the weight windows is based on an external mesh superimposed on the Monte Carlo model. The window bounds can be based on several kinds of importance maps: the ones produced by the built-in importance map generator INIPOND of TRIPOLI-4, external maps produced by the deterministic solver IDT provided with TRIPOLI-4, or by the output of a version 3.0 of ADVANTG deterministic code (directly through a so-called wwinp file) [72].

TRIPOLI-4 automatically applies importance values on the source (i.e. source biasing), to simulate source particles with emission statistical weights already in agreement with the weight windows data that apply to the related source area. These importance values are retrieved from the adjoint fluxes or derived from the lower bounds weight data.

Weight windows have been tested against other variance-reduction methods of TRIPOLI-4 and other Monte Carlo codes. For illustration, the comparison of several variance-reduction methods of TRIPOLI-4 applied to dose calculations for a spent-fuel assembly transport cask [69] is displayed in Figure 11.

3.3 Adaptive Multilevel Splitting (AMS)

In order to further widen the spectrum of variance-reduction methods available to the users, TRIPOLI-4 has been also endowed with the Adaptive Multilevel Splitting (AMS) method, a variance-reduction technique based on importance-weighted particle splitting [73,74] that provides a valuable alternative to the legacy exponential transform or to weight windows [75–78].

AMS relies on an iterative process that is performed in each batch (replica) of the simulation. Within a single iteration, particle transport sampling is set to analog: particle trajectories are simulated without applying importance sampling, or standard variance-reduction techniques

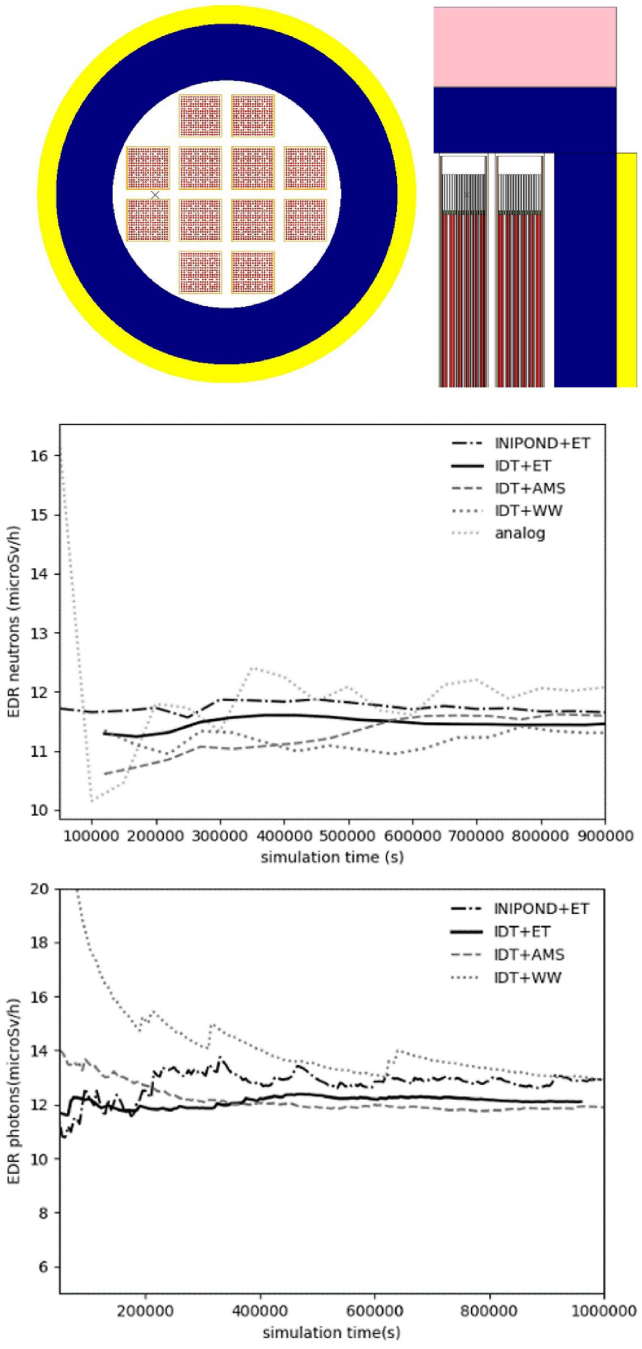

Fig. 11. Comparison of several variance-reduction methods of TRIPOLI-4 for a benchmark configuration consisting of a transport cask for spent-fuel assemblies. The fiducial quantity to be assessed is the Equivalent Dose Rate (EDR) at 2 meters from the package, at mid-height. Top: radial and axial (zoom) cutoff of the benchmark model, with resin in yellow, steel shell in dark blue, and shock absorbers in pink. Center and bottom: analysis of the convergence patterns of neutron (resp. photon) EDR as a function of the simulation time (proportional to the number of replicas). The tested methods are exponential transform with INIPOND map (INIPOND+ET) or with IDT map (IDT+ET), AMS with IDT map (IDT+AMS), and weight windows with IDT map (IDT+WW). Figure adapted from reference [69]. (This figure is subject to copyright protection and is not covered by Creatice Commons License. SNA+MC, 2024).

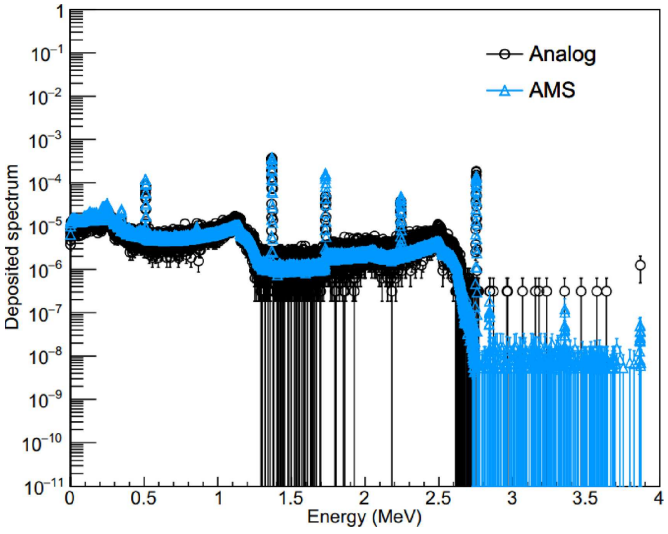

Fig. 12. Application of the AMS variance-reduction method to the calculation of the deposited spectrum in a HPGe detector, for a benchmark configuration. Comparison between simulations with (blue) and without (black) AMS. Figure taken from reference [76]. (This figure is subject to copyright protection and is not covered by Creatice Commons License. EDP Sciences, 2017).

such as implicit capture[6]. Then, particles are sorted with respect to the maximum of a user-provided importance map (referring to a detector region) evaluated along the trajectories.

The importance map can be of several kinds: a pure geometrical map (based on volumes, surfaces, or paths) [79], the space/energy map produced by the built-in INIPOND importance map generator of TRIPOLI-4, or an external adjoint-based importance map produced by IDT [68].

For each iteration of the algorithm, the sorting process allows setting a 'splitting level', which adaptively singles out the particles having the highest importance. All trajectories below the splitting level are removed from the simulation, and re-sampled by duplicating some of the best-ranked trajectories at their crossing of the current splitting level. The fraction of particles to be split at each AMS iteration is set by the users. In order to reduce the impact of correlations, by default the splitting rate per iteration is 1% and in any case, it should not exceed 50%. The iterations of the AMS method progressively promote particles to the detector region, and this procedure is unbiased [73,74].

AMS can be used for both single-particle transport problems and for coupled transport problems including neutrons and photons, or photons, electrons, and positrons in the electromagnetic shower. It can be also used together with gamma spectrometry tallies. For illustration, Figure 12 shows an application to the calculation of the deposited spectrum in a HPGe detector [76].

[6] Optionally, implicit capture can be activated.

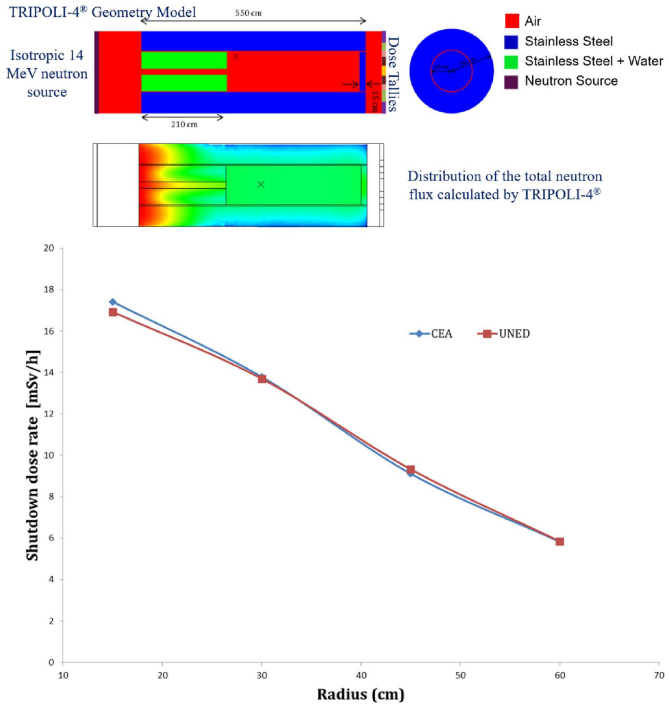

Fig. 13. Application of the R2S to the calculation of the dose in the ITER port-plug benchmark. The variance reduction required for the flux calculation has been achieved using the INIPOND built-in module. Top: scheme of the Monte Carlo model and neutron distribution computed with TRIPOLI-4. Bottom: The dose estimation obtained with TRIPOLI-4 at several positions within the port plug is compared to analogous results obtained by the UNED (Spain). Figure adapted from reference [80]. (This figure is subject to copyright protection and is not covered by Creatice Commons License. EDP Sciences, 2017).

3.4 Activation calculations: R2S

The goal of activation calculations is typically to compute the dose delivered by photons due to the decay of material compositions that underwent neutron activation. TRIPOLI-4 can compute shutdown dose rates including neutron and photon contributions, based on a Rigorous 2-step Scheme (R2S) [80] that relies on the MENDEL solver [10].

The two 'steps' of the R2S calculation are the following. In the first step, neutrons are transported throughout the geometry, and the associated neutron fluxes and reaction rates are tallied. The fluxes and reaction rates feed the source term of a system of Bateman equations for the concentrations of all the possible activation products. The Bateman equations are then numerically solved using the MENDEL solver, and the activities are determined at all the requested times. The neutron flux is allowed to vary in intensity over the activation time range, but it is assumed that the shape of the flux does not change (a single neutron transport calculation is necessary).

In the second step, for each activation time, the photon spectra emitted by the activation products are computed by MENDEL, and fed to TRIPOLI-4 as the source for a photon-transport calculation. Contrary to depletion calculations, the neutron flux and the reaction rates are not homogenized over the volumes of the Monte Carlo model. The user defines a mesh over the region of interest for activation and specifies the materials whose activation needs to be considered. Each mesh cell is then separately activated and represents a distinct radiation source for the second calculation step.

For illustration, the application of the R2S scheme to the calculation of the dose within the ITER port-plug benchmark [80] is shown in Figure 13. Both steps of the R2S scheme may be run in parallel, using the standard parallelism scheme of TRIPOLI-4. Additionally, TRIPOLI-4 offers the possibility to parallelize the solution of the Bateman equations using OpenMP.

Since R2S calculations are very similar to depletion calculations, one should apply the same caveats concerning the calculation of the statistical uncertainties on the calculation results. A single two-step calculation (neutron activation and photon transport) cannot yield any estimate of the uncertainty. The only rigorous way to estimate the uncertainty is to observe a number of independent calculation replicas. One can then estimate the standard error from the dispersion of the sample.

4 Nuclear instrumentation applications

Finally, in this section, we describe the new features of TRIPOLI-4 concerning nuclear instrumentation applications.

4.1 Electromagnetic shower models

The simulation of the electromagnetic shower (coupled photon, electron, and positron transport) has a largely higher computational cost than pure photon simulation. Nonetheless, pure photon transport underestimates the secondary photon production at high energy, since bremsstrahlung photons are not sampled if electrons are not simulated. As a compromise, similarly to what is done in other Monte Carlo codes [81], in order to improve the accuracy of TRIPOLI-4 without taking into account the full electromagnetic shower, we have developed the Thick-Target Bremsstrahlung (TTB) model [82,83], a simplified sampling scheme that replaces electron emission and propagation by the (approximate) emission of secondary bremsstrahlung photons [84,85]. The hypothesis used in the TTB model is more appropriate for thick material regions [81], which explains the acronym of the model. Contrary to the standard implementation of MCNP [81], TRIPOLI-4 takes into account the angular straggling of the condensed electrons. For illustration, results of the application of the TTB model [85] are shown in Figure 14.

The electromagnetic shower models available in TRIPOLI-4 have been updated [84,85]. In previous versions of TRIPOLI-4, the legacy model for the production of bremsstrahlung photons by electrons and positrons was the one developed by Berger and Seltzer in 1970 [86]. In

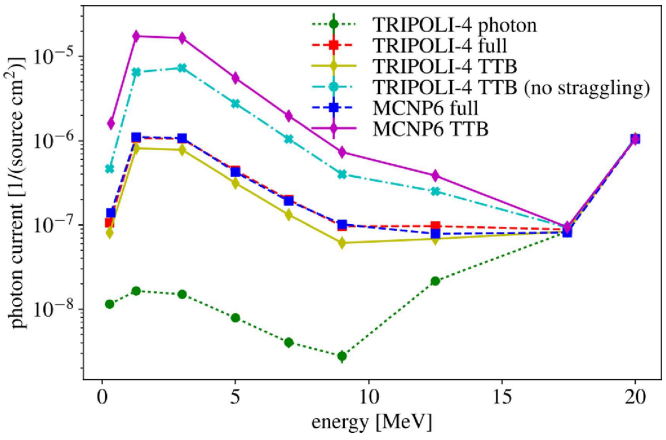

Fig. 14. Energy spectrum of photons transmitted through a thick lead slab: comparison of TRIPOLI-4 and MCNP results, with and without TTB model. For TRIPOLI-4, we additionally show results with TTB but without electron angular straggling. Figure taken from reference [85]. (This figure is subject to copyright protection and is not covered by Creatice Commons License. IEEE, 2018).

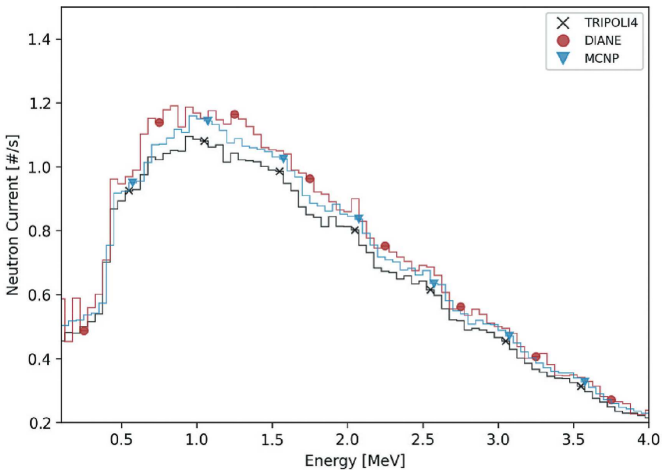

Fig. 15. Comparison of photo-neutron yield spectra of the Barber and George benchmark, as computed by TRIPOLI-4 (crosses), DIANE [98] (circles), and MCNP6 [81] (triangles) for a Pb target with an electron source energy of 34.5 MeV. Figure adapted from reference [97]. (This figure is subject to copyright protection and is not covered by Creatice Commons License. Taylor & Francis, 2024).

the current version of the code, by default, we use instead a newer state-of-the-art model for energy-differential cross sections developed by the same authors [87], based on the interpolation of tabulated values derived from numerical phase-shift calculations for electron energies lower than 2 MeV, and from the analytical high-energy theory above 50 MeV (the intermediate energy region is covered by interpolating between the two other regions).

The inelastic collisions leading to secondary electrons above the transport threshold are explicitly handled in TRIPOLI-4, using a 'Class I' algorithm [85]: electron tracks are assumed to lose a constant fraction (0.02) of their kinetic energy along each step, on an average. The energy loss at each step is directly mirrored in the maximum length of the electron displacement. The actual steps may be smaller than the upper limit whenever electrons undergo hard collisions or cross a geometrical boundary: for this reason, TRIPOLI-4 automatically refines electron steps close to the cell boundaries (the minimum allowed step size is a user-defined parameter).

In TRIPOLI-4, electron angular straggling follows the Goudsmit-Saunderson model [88], which is used to condense elastic cross sections from several models and tables: at 256 keV and below, the code uses data from the Evaluated Electron Data Library (EEDL) [89], which provides integrated and angle-differential large-angle elastic cross sections; above 256 keV, the code uses the Mott cross section [90] with Molière's screening correction [91,92], as computed by Feshbach [93] and Sherman [94]. These models have been benchmarked against other Monte Carlo codes and the processing of the cross sections has been in particular fixed below 256 keV [85].

Furthermore, we have added the capability of estimating the charge deposition distribution in collectrons (self-powered neutron and gamma detectors), which are passive devices for in-core measurement of neutron and/or gamma flux. The charge deposition is required in order to characterize the response of such instruments. The estimator implemented in TRIPOLI-4 relies on the accumulation of positive and negative increments to the charge deposition whenever a charged particle is born or dies in the considered region.

4.2 Photo-nuclear reactions

Models and kinematics for photo-nuclear reactions in TRIPOLI-4 have been revisited, and minor issues have been fixed, especially in connection with the compatibility with modern nuclear data libraries, such as ENDF/B-VIII [95] or JENDL-5 [96]. Photo-nuclear reactions have been extensively validated by comparison with respect to experimental measurements (using in particular the Barber and George benchmark) and other Monte Carlo codes [97]: for illustration, the case of photo-neutron spectra produced on a lead target irradiated with high-energy electrons is shown in Figure 15.

4.3 Charged particle transport

TRIPOLI-4 lacks the native capability of transporting charged particles heavier than electrons and positrons. Many of these particles, such as protons and alphas, are of interest in nuclear instrumentation, as well as in decommissioning and radiation shielding applications. In view of coping with these issues, TRIPOLI-4 has been coupled to Geant4 [99], a particle-transport toolkit developed by several institutions around the world, offering a large spectrum of physical models for the simulation of particle-matter interactions. Although some development efforts are ongoing, Geant4 generally lacks variance-reduction methods and most of its models are based on analog sampling, which makes the code inefficient for typical radiation shielding problems with strong attenuation and/or

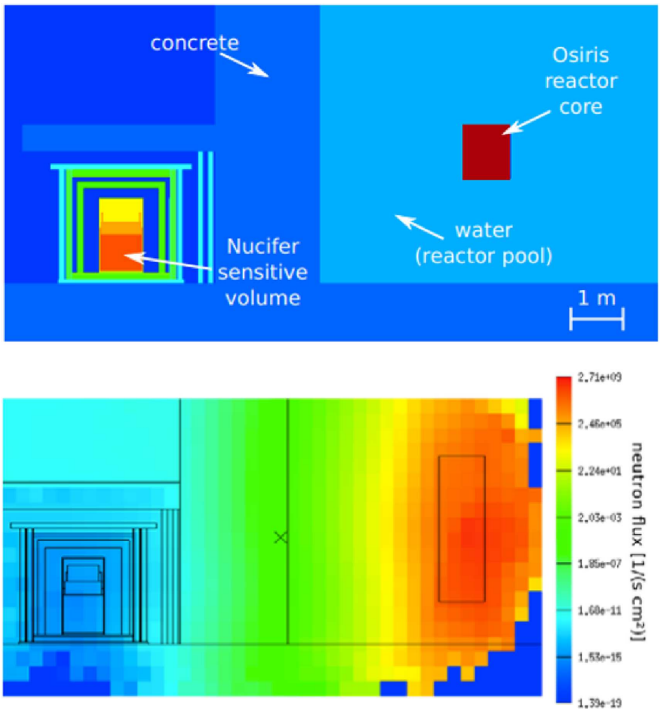

Fig. 16. Application of the coupling of TRIPOLI-4 with Geant4 for the simulation of the Nucifer-Osiris configuration. Top: Cross section of the setup of the Nucifer-Osiris configuration. Bottom: The neutron flux in the 8–20 MeV energy group, as computed by TRIPOLI-4 in the Nucifer model of Geant4. Figure adapted from reference [100]. (This figure is subject to copyright protection and is not covered by Creatice Commons License. EDP Sciences, 2017).

obstacles. In this respect, Geant4 and TRIPOLI-4 (which is on the contrary endowed with a large spectrum of variance-reduction methods) complement each other fairly well. The coupling between TRIPOLI-4 and the Geant4 makes it possible for users to tap into Geant4 physics library and use TRIPOLI-4 to solve transport problems that involve charged particles. Additionally, TRIPOLI-4 can use Geant4 geometries just like another geometry format (similar to what is done for ROOT geometries). For illustration, an application to the calculation of the neutron flux in the Nucifer-Osiris configuration [100] is displayed in Figure 16.

4.4 Analog simulation and fission models

TRIPOLI-4 can simulate fully analog neutron and photon transport, without any variance-reduction method [101–104]. This simulation mode is useful for applications in nuclear instrumentation where one is concerned with the correlations between particle-induced events (in space, energy, or time), including those related to fission chains. In the current version of the code, coupled neutron/photon analog transport is not available, since analog photon production induced by neutron interactions has not been implemented, yet.

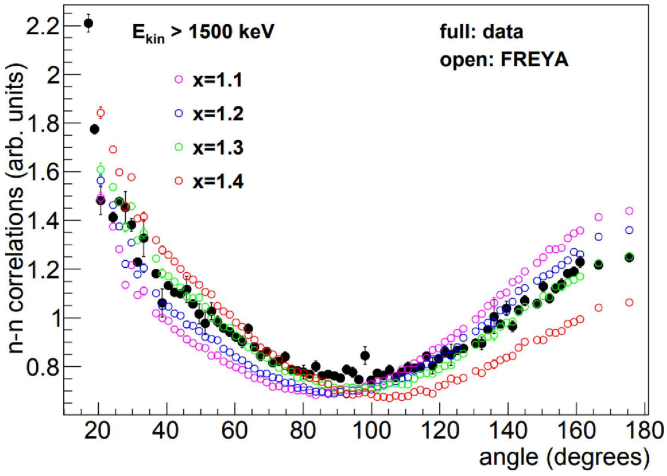

Fig. 17. Two-neutron angular correlation for the spontaneous fission of ^{240}Pu as a function of the angular separation and for a neutron kinetic energy threshold of 1500 keV. Comparison between experimental data (full symbols) and FREYA (open symbols) calculations, shown for several values of the parameter x that defines the partition of the excitation energy between the light and heavy fission fragments. Figure taken from reference [101]. (This figure is subject to copyright protection and is not covered by Creatice Commons License. IEEE, 2018).

For neutrons, a key ingredient of analog Monte Carlo simulations is the 'fission model' used to sample the descendant neutrons emitted at fission events: for this purpose, TRIPOLI-4 relies on either FREYA (Fission Reaction Event Yield Algorithm) [105], developed at Lawrence Livermore National Laboratory, or FIFRELIN [106], developed at CEA/Cadarache. Based on the chosen model, TRIPOLI-4 samples from the neutron multiplicity distribution, instead of using the average multiplicity as in regular non-analog simulations with standard evaluated data.

The use of FREYA requires that the users download the LLNL Fission Library package[7]. During the simulation, FREYA is called by TRIPOLI-4 at each collision with a fissile nuclide, and the event-by-event fission model is used to sample the post-collision features of the emitted neutrons. Spontaneous fission can be also modeled, defining an external source that directly calls FREYA. For illustration, an application to the analysis of correlations in the spontaneous fission of ^{240}Pu is illustrated in Figure 17. FIFRELIN is used differently: before running TRIPOLI-4, specific 'event files' are produced by FIFRELIN for a given fissile nuclide, each being valid for a given energy domain. The files are then stored and read by TRIPOLI-4 during the simulation. Similarly, as for FREYA, spontaneous fission can be also taken into account.

Tallies specific to analog transport have been developed. The fission multiplicity and spectra can be scored (as a function of energy), as sampled during the simulation using fission models. Furthermore, the distribution of the Z (charge number) and A (mass number) of the fission

[7] http://nuclear.llnl.gov/simulation/

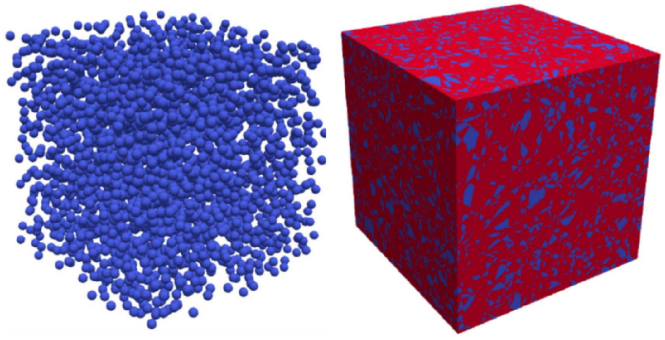

Fig. 18. Examples of three-dimensional random media realizations sampled using CASTOR. Left: random spherical inclusions with mono-dispersed radii. Right: Markov media based on isotropic and spatially homogeneous Poisson tessellations with binary coloring.

fragments produced at fission events can be also scored, and are then edited in the form of a two-dimensional histogram over a user-defined mesh.

Finally, analog simulation is usefully complemented by the analysis of the sampled particle tracks, which can be stored and post-processed via the ROOT TRACKS option of TRIPOLI-4 based on the coupling with ROOT.

5 Geometry models

5.1 Random media sampler: CASTOR

TRIPOLI-4 is endowed with the external tool CASTOR (Construction and Analysis of STOchastic Realizations), a random media Monte Carlo sampler that has been developed to generate three types of three-dimensional stochastic geometries [107]: isotropic and homogeneous Poisson tessellations, Poisson-Box tessellations, and three-dimensional spherical inclusions (non-overlapping spheres with low packing-fraction) in a background matrix. The spheres of the spherical inclusions can be either mono-dispersed (constant radius) or poly-dispersed (radius sampled according to a probability law). For illustration, some examples of random media sampled with CASTOR are displayed in Figure 18.

For Poisson and Poisson-Box tessellations, a 'coloring' procedure is performed after the sampling of the cells of the skeleton geometry [108,109]: each cell of the tessellation is assigned a color label α with a probability p_α, $\alpha = 1, \ldots, n$. The resulting stochastic configurations form isotropic or anisotropic random n-ary Markov mixtures (collections of material compositions whose geometrical shapes obey a given probability distribution), and provide convenient models to describe complex systems such as corium following severe accidents, or turbulent layers in fusion pellets [110]. For spherical inclusions, binary mixtures result from the sampling (the sphere and the background matrix), with a given packing fraction: such configurations might be used e.g. to model the fuel elements of HTR reactors [111].

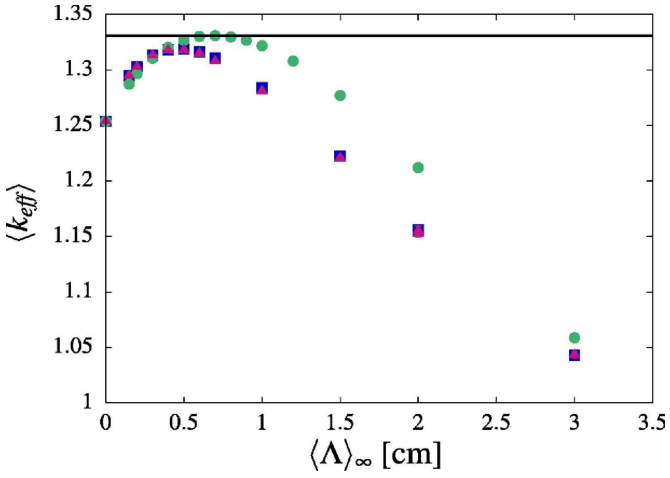

Fig. 19. Comparison of excess reactivity in a UOX assembly due to fuel degradation, as described by different random media models (Poisson tessellations in blue squares, Poisson-Box tessellations in red triangles, and Voronoi tessellations in green circles). The average multiplication factor is shown as a function of the typical length scale of the fuel randomization. Figure taken from reference [112]. (This figure is subject to copyright protection and is not covered by Creatice Commons License. Elsevier, 2018).

For each of the available random media models, CASTOR samples an ensemble of N realizations, compatible with the format expected by TRIPOLI-4 (including the geometry, the boundary conditions, and the association between cells and material compositions). For each realization, a TRIPOLI-4 simulation is run and a set of observables is estimated. The histogram over the set of performed simulations allows computing the average and the dispersion of the sought results (the dispersion is due to both the variance of the underlying stochastic media and the statistical dispersion of the Monte Carlo simulations). An example of application to the analysis of the excess reactivity due to UOX fuel assembly degradation [112] is shown in Figure 19. Reference solutions for particle transport computed by taking an ensemble over a large collection of random media realizations can be used to benchmark results obtained with faster-homogenized models such as the Chord Length Sampling method [116,117].

5.2 Connectivity maps

TRIPOLI-4 is endowed with the capability of producing connectivity maps, i.e., tables of matrix indices that describe the nearest neighborhood of each cell of the Monte Carlo model, in view of optimizing the performance of particle tracking during simulation. For combinatorial geometries, the neighborhood map is automatically built during the initialization of the geometrical model, whereas for surface-based geometries the map is filled during the simulation: particles progressively explore the viable space and store the cells seen by their trajectories.

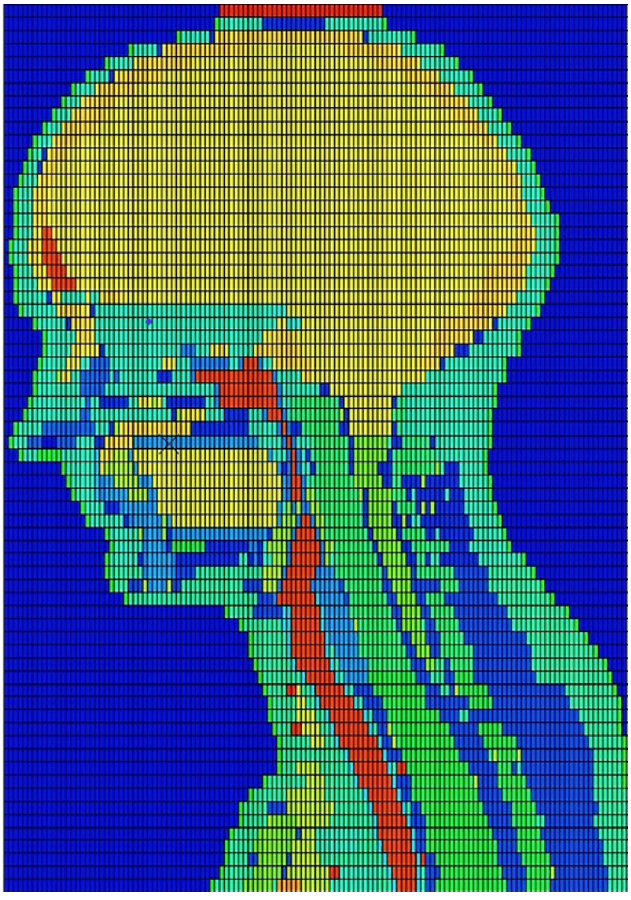

Fig. 20. Cut along the y-z axes of the TRIPOLI-4 model (zoom) of the ICRP 110 voxel phantom Laura. The visualization is obtained using the T4G voxel contour option. Figure taken from reference [118]. (This figure is subject to copyright protection and is not covered by Creatice Commons License. ASME, 2020).

In either case, particle exploration during subsequent replicas (or fission cycles for power iteration) reinforces the map, in that the visit frequency for each cell is used to further promote the search of the next-crossed surface for particle tracking. The neighborhood maps thus produced can be stored and reused for other calculations. The maps need not to be exhaustive and complete, since TRIPOLI-4 will take care of filling the empty elements. Furthermore, the wrong attribution of a neighborhood index will not induce errors in particle tracking: after trying and failing to locate the next cell visited according to a wrong index, TRIPOLI-4 will fall back on general research over the next neighbors. Connectivity maps are available in both single-processor and parallel modes.

Several tests have shown that optimized connectivity maps can speed up calculations by substantial factors, especially for complex models composed of hundreds of thousands of cells, such as large reactor cores with detailed pin-by-pin descriptions, or large stochastic media composed of millions of tiny cells [113–115].

5.3 Voxelized geometries

The capability of dealing with voxelized geometries has been developed in TRIPOLI-4, mainly for the needs of radiation shielding and dosimetry applications. For this purpose, preliminary attempts have been based on the existing lattice description in combinatorial geometry [118], which is commonly used for reactor physics configurations. Satisfactory performances have been achieved e.g. for the Laura voxel phantom of ICRP 110, including more than 1.4×10^7 voxels: for an illustration, see Figure 20. Furthermore, in order to improve the performances of both particle tracking and visualization with T4G for large voxelized geometries, two major modifications have been implemented [119]: the first concerns a careful use of operators in the combinatorial geometry so to reserve the voxel phantom space in the background environment; the second concerns the reorganization of data structures of the involved array. Tests conducted in large voxel phantoms have shown that the combination of both modifications leads to gains of the order of 100 on the time required for particle tracking, and even larger for the visualization. Voxelized geometries are currently under extensive testing and validation, mainly in the context of the participation to the EURADOS consortium [120,121], and will be integrated in a future release of TRIPOLI-4.

6 Conclusions and perspectives

In this paper we have described the major developments achieved in the Monte Carlo code TRIPOLI-4 over the last decade, spanning a broad range of applications in the domains of reactor physics, criticality safety, radiation shielding, and nuclear instrumentation. For each development, verification, and validation tests have been also briefly detailed. Most of these capabilities are already available in the current release, version 12 of TRIPOLI-4, but we have also mentioned current R&D on some functionalities that will be soon integrated in the next official release.

Future work will be aimed at extending the domain of applicability of TRIPOLI-4 in several directions. The implementation of the CADIS method will be extended to cover coupled neutron/photon transport simulations; furthermore, the Forward-Weighted CADIS method [122] will be also implemented to achieve global variance reduction. Geometry engines will be expanded by taking into account particle tracking in CAD-generated geometries, whose preliminary investigation is ongoing. The CASTOR random media sampler will be generalized to include spatial gradients, which often occur in real-world applications due to material stratification [123]. Efficient variance-reduction and population-control methods for time-dependent simulations are under investigation, in order to achieve considerably higher figures of merit for this class of highly CPU-intensive calculations [125]. Similar efforts are underway for GPT sensitivities of the effective delayed neutron fraction with respect to nuclear data [124], which is also highly demanding in terms of computer resources. Finally, extensive work has been recently

carried out on Monte Carlo methods for solving the neutron noise equation in the frequency domain [126,127]: the basic implementation has been successfully tested in the development version of TRIPOLI-4, in the framework of the European H2020 project CORTEX, and further investigations concerning distinct variance-reduction methods based on statistical weight annihilation are ongoing [128].

Acknowledgments

TRIPOLI-4 is a registered trademark of CEA.

Funding

The authors thank EDF for partial financial support.

Conflicts of interest

The authors declare that they have no competing interests to report.

Data availability statement

No data are associated with this manuscript.

Author contribution statement

All authors contributed to the development and implementation of the technical work described in this manuscript. The writing was coordinated by A. Zoia. All authors proofread the final version of the paper.

References

1. E. Brun et al., TRIPOLI-4, CEA, EDF and AREVA Reference Monte Carlo Code, Ann. Nucl. Energy **82**, 151 (2015)
2. J.P. Both, H. Derriennic, B. Morillon, J.C. Nimal, A survey of TRIPOLI-4, in *Proc. 8th Intl. Conf. Rad. Shield., Arlington USA*, (1994), p. 373
3. V. McLane, ENDF-102 Data Formats and Procedures for the Evaluation Nuclear Data File ENDF-6. Technical report BNL-NCS-44945-01/04-REV, Brookhaven National Laboratory, USA, 2004
4. J.C. Sublet, P. Ribon, M. Coste-Delclaux, CALENDF-2010: User manual, Technical report CEA-R-6277, CEA, France, 2011
5. A. Zoia, E. Brun, C. Jouanne, F. Malvagi, Doppler broadening of neutron elastic scattering kernel in TRIPOLI-4, Ann. Nucl. Energy **54**, 218 (2013)
6. R. Brun, F. Rademakers, ROOT, an object-oriented data analysis framework, Nucl. Instrum. Methods A **389**, 81 (1997)
7. J.P. Both, Y. Pénéliau, Parallelization of the Monte Carlo code TRIPOLI-4, in *Proc. of M&C99, Madrid, Spain*, (1999)
8. Y.K. Lee, F.X. Hugot, TRIPOLI-4 Neutron Multiplication Calculations for the Subcritical Experiments of the BeRP Ball Reflected by Tungsten, in *Proc. of ICNC 2023, The 12th Int. Conf. on Nuclear Criticality Safety, Sendai, Japan*, (2023)
9. E. Brun, A. Zoia, J.C. Trama, S. Lahaye, Y. Nagaya, Inter-code comparison of TRIPOLI and MVP on the MCNP criticality validation suite, in *prof. of ICNC-2015, International Conference on Nuclear Criticality Safety, Charlotte*, USA, (2015)
10. S. Lahaye et al., New Bateman Equation Solvers in MENDEL version 3.1, in *Proc. ICNC2023, Sendai, Japan*, (2023)
11. G. Dejonghe, J. Gonnord, J.C. Nimal, Perturbation calculations by the correlated samples method, in *Proc. of the Intl. Meeting on Advances in Nuclear Engineering Computational Methods, Knoxville, USA*, (1985)
12. H. Rief, Generalized Monte Carlo perturbation algorithm for correlated sampling and a second-order Taylor series approach, Ann. Nucl. Energy **11**, 455 (1984)
13. S. Bourganel, O. Petit, C.M. Diop, Three-dimensional particle transport using Green's functions in TRIPOLI-4 Monte Carlo code: application to PWR neutron fluence and ex-core response studies, Nucl. Technol. **184**, 29 (2013)
14. J.P. Both, J.C. Nimal, T. Vergnaud, Automated importance generation and biasing techniques for Monte Carlo shielding techniques by the TRIPOLI-3 code, Prog. Nucl. Energy **24**, 273 (1990)
15. O. Petit et al., Variance reduction adjustment in Monte Carlo TRIPOLI-4 neutron gamma coupled calculations, Prog. Nucl. Sci. Technol. **4**, 408 (2014)
16. F.X. Hugot, Y.K. Lee, A new prototype display tool for the Monte Carlo particle transport code TRIPOLI-4, Prog. Nucl. Sci. Technol. **2**, 851 (2011)
17. Y.K. Lee, F.X. Hugot, TRIPOLI-4 Monte Carlo Code Verification and Validation using T4G Tool, in *Proc. of ICONE 31, 31st Int. Conf. on Nuclear Engineering, Prague, Czech Republic*, (2024)
18. E. Le Ménédeu, D. Mancusi, Valjean, a universal post-processing tool for neutronics, in *Proc. of SNA+MC2024, Paris, France*, (2024)
19. D. Mancusi, Automatic Conversion of MCNP Geometries to TRIPOLI-4, in *Proc. of Physor 2022, Pittsburgh, USA*, (2022)
20. Y.K. Lee, TRIPOLI-4 calculations of neutron multiplicity counting rates of He-3 array detectors and verification tests of an automatic MCNP-to-TRIPOLI conversion tool for recent ICSBEP subcritical experiments, in *Proc. of SNA+MC2024, Paris, France*, (2024)
21. D. Mancusi et al., Overview of TRIPOLI-5, a Monte Carlo code for HPC, to be submitted to EPJ Nuclear Sci. Technol. (to be published)
22. A. Jinaphanh, A. Zoia, Computing adjoint-weighted tallies with TRIPOLI-4 using the Wielandt method, in *Proceedings of M&C2019, Portland, USA*, (2019)
23. F. Filiciotto, A. Jinaphanh, A. Zoia, Super-history methods for adjoint-weighted tallies in Monte Carlo time eigenvalue calculations, in *Proceedings of Physor2020, Cambridge, UK*, (2020)
24. T. Yamamoto, Y. Miyoshi, Reliable method for fission source convergence of Monte Carlo criticality calculation with Wielandt's method, J. Nuclear Sci. Technol. **41**, 99 (2004)
25. R.J. Brissenden, A.R. Garlick, Biases in the estimation of Keff and its error by Monte Carlo methods, Ann. Nucl. Energy **13**, 63 (1986)
26. Y. Qiu et al., Computing eigenvalue sensitivity coefficients to nuclear data by adjoint superhistory method and adjoint Wielandt method implemented in RMC code, Ann. Nucl. Energy **87**, 228 (2016)

27. N. Terranova, G. Truchet, I. Zmijarevic, A. Zoia, Adjoint neutron flux calculations with TRIPOLI-4: Verification and comparison to deterministic codes, Ann. Nucl. Energy **114**, 136 (2018)
28. S. Carney, F. Brown, B. Kiedrowski, W. Martin, Theory and applications of the fission matrix method for continuous-energy Monte Carlo, Ann. Nucl. Energy **73**, 423 (2014)
29. Y.K. Lee, A. Monnier, J.P. Both, J.C. Nimal, Benchmark Validation of the Criticality Code TRIMARAN2 (TRIPOLI-4 multi-group option), in *Proc. of ICNC'95, The Fifth Int. Conf. on Nuclear Criticality Safety, Albuquerque, USA*, (1995), p. 3.12
30. V. Vitali et al., Eigenvalue separation and eigenmode analysis by matrix-filling Monte Carlo methods, Ann. Nucl. Energy **164**, 108563 (2021)
31. M. Mancusi, A. Zoia, Chaos in eigenvalue search methods, Ann. Nucl. Energy **112**, 354 (2018)
32. Y. Nauchi, T. Kameyama, Development of calculation technique for iterated fission probability and reactor kinetic parameters using continuous-energy Monte Carlo method, J. Nuclear Sci. Technol. **47**, 977 (2010)
33. B.C. Kiedrowski, F.B. Brown, P.P.H. Wilson, Adjoint-weighted tallies for k-eigenvalue calculations with continuous-energy Monte Carlo, Nucl. Sci. Eng. **168**, 226 (2011)
34. G. Truchet, P. Leconte, A. Santamarina, E. Brun, F. Damian, A. Zoia, Computing adjoint-weighted kinetics parameters in TRIPOLI-4, Ann. Nucl. Energy **85**, 17 (2015)
35. A. Zoia, E. Brun, Reactor physics analysis of the SPERT III E-core with TRIPOLI-4, Ann. Nucl. Energy **90**, 71 (2016)
36. A. Zoia, Y. Nauchi, B. Brun, C. Jouanne, Monte Carlo analysis of the CROCUS benchmark on kinetics parameters calculation, Ann. Nucl. Energy **96**, 377 (2016)
37. A. Zoia, C. Jouanne, P. Siréta, P. Leconte, G. Braoudakis, L. Wong, Analysis of dynamic reactivity by Monte Carlo methods: the impact of nuclear data, Ann. Nucl. Energy **110**, 11 (2017)
38. N. Terranova, D. Mancusi, A. Zoia, New perturbation and sensitivity capabilities in TRIPOLI-4, Ann. Nucl. Energy **121**, 335 (2018)
39. A. Jinaphanh, A. Zoia, Perturbation and sensitivity calculations for time eigenvalues using the generalized iterated fission probability, Ann. Nucl. Energy **133**, 678 (2019)
40. A. Jinaphanh, C. Carabajal, A. Zoia, Implementation and Testing of the GPT Sensitivities. in TRIPOLI-4, in *Proc. of Physor 2022, Pittsburgh, USA*, (2022)
41. A. Jinaphanh, P. Dufour, A. Zoia, Computing the sensitivity of effective kinetics parameters by Monte Carlo methods using a super-history approach, in *Proceedings of M&C2023, Niagara Falls, Canada*, (2023)
42. A. Jinaphanh, G. Valocchi, A. Zoia, Implementation and testing of generalized perturbation Theory capabilities in TRIPOLI-4, Nucl. Sci. Eng., 1 (2024)
43. B.C. Kiedrowski, F.B. Brown, Adjoint-based k-eigenvalue sensitivity coefficients to nuclear data using continuous-energy Monte Carlo. Nucl. Sci. Eng. **174**, 227 (2013)
44. T.P. Burke, B.C. Kiedrowski, Monte Carlo perturbation theory estimates of sensitivities to system dimensions, Nucl. Sci. Eng. **189**, 199 (2018)
45. G. Shi et al., Improved generalized perturbation theory method for sensitivity analysis of generalized response function, Prog. Nucl. Energy **134**, 103643. (2021)
46. M. Faucher, D. Mancusi, A. Zoia, New kinetic simulation capabilities for TRIPOLI-4: methods and applications, Ann. Nucl. Energy **120**, 74 (2018)
47. E. Dumonteil et al., Particle clustering in Monte Carlo criticality simulations, Ann. Nucl. Energy **63**, 612 (2014)
48. B. Houchmandzadeh, E. Dumonteil, A. Mazzolo, A. Zoia, Neutron fluctuations: The importance of being delayed, Phys. Rev. E **92**, 052114 (2015)
49. T. Bonnet, D. Mancusi, A. Zoia, Space and time correlations for diffusion models with prompt and delayed birth-and-death event, Phys. Rev. E **105**, 064105 (2022)
50. M. Faucher, D. Mancusi, A. Zoia, Variance-reduction methods for Monte Carlo kinetic simulation, in *Proc. M&C 2019, Portland, USA*, (2019)
51. B.L. Sjenitzer, J.E. Hoogenboom, Dynamic Monte Carlo method for nuclear reactor kinetics calculations, Nucl. Sci. Eng. **175**, 94 (2013)
52. T. Bonnet, H. Belanger, D. Mancusi, A. Zoia, The effect of branchless collisions and population control on correlations in Monte Carlo power iteration, Nucl. Sci. Eng. 1 (2024)
53. T. Booth, A weight (charge) conserving importance-weighted comb for Monte Carlo, in *Proc. RPSD Topical Meeting, Falmouth, USA*, (1996)
54. D. Mancusi, A. Zoia, Zero-variance schemes for kinetic Monte Carlo simulations, Eur. Phys. J. Plus **135**, 401 (2020)
55. O. Petit, C. Jouanne, Stochastic temperature interpolation in the Monte Carlo code TRIPOLI-4, in *Proc. of SNA+MC 2020, Chiba, Japan*, (2020)
56. R. MacFarlane, D. Muir, The NJOY Nuclear Data Processing System, version 91, Technical report LA12740-M, Los Alamos National Laboratory, USA, 1994
57. M. Faucher et al., Multi-physics simulations with TRIPOLI-4: coupling neutron transport with the CFD code TRUST/TrioCFD, in *Proc. ICAPP2019, Juan-les-pins, France*, (2019)
58. D. Ferraro et al., Serpent and TRIPOLI-4 transient calculations comparisons for diverse reactivity insertion scenarios in a 3D PWR minicore benchmark, in *Proc. M&C2019, Portland, USA*, (2019)
59. M. Faucher, D. Mancusi, A. Zoia, Multi-Physics Transient Simulations With TRIPOLI-4, EPJ Web Conf. **247**, 07019 (2021)
60. D. Mancusi, M. Faucher, A. Zoia, Monte Carlo simulations of the SPERT III E-core transient experiments, Eur. Phys. J. Plus. **137**, 127 (2022)
61. U. Imke, V.H. Sanchez, Validation of the Subchannel Code SUBCHANFLOW Using the NUPEC PWR Tests (PSBT), Sci. Technol. Nucl. Install. **2012**, 465059 (2012)
62. J.C. Wagner, A. Haghighat, Automated variance reduction of Monte Carlo shielding calculations using the discrete ordinates adjoint function, Nucl. Sci. Eng. **128**, 186 (1998)
63. A. Haghighat, J.C. Wagner, Monte Carlo variance reduction with deterministic importance functions, Prog. Nucl. Energy **42**, 25 (2003)
64. M. Munk, R.N. Slaybaugh, Review of hybrid methods for deep-penetration neutron transport, Nucl. Sci. Eng. **193**, 1055 (2019)

65. M. Nowak et al., Accelerating Monte Carlo shielding calculations in TRIPOLI-4 with a deterministic adjoint flux, Nucl. Sci. Eng. **193**, 966 (2019)
66. D. Mancusi et al., Evaluating importance maps for TRIPOLI-4 using deterministic or on-line methods, in *Proc. RPSD2018, Santa Fe, USA*, (2018)
67. I. Zmijarevic, R. Sanchez, Deterministic solutions for 3D Kobayashi benchmarks, Prog. Nucl. Energy **39**, 207 (2001)
68. M. Falabino et al., Comparison of variance reduction methods in shielding problems with source multiplication, Eur. Phys. J. Plus **136**, 598 (2021)
69. A. Bonin, O. Petit, Efficiency of variance-reduction techniques using TRIPOLI-4: application to equivalent dose rate calculations in a spent fuel cask, in *Proc. of SNA+MC2024, Paris, France*, (2024)
70. T.E. Booth, Genesis of the Weight Window and Weight Window Generator in MCNP – A Personal History, Technical Report LA-UR-06-5807, Los Alamos National Laboratory, 2006
71. J. Sweezy, F.B. Brown, T. Booth, J. Chiaramonte, B. Preeg, Automated variance reduction for MCNP using deterministic methods, Radiat. Prot. Dosimetry **116**, 508 (2005)
72. S. Mosher et al., ADVANTG – An Automated Variance Reduction Parameter Generator, Technical report ORNL/TM-2013/416 Rev. 1, Oak Ridge National Laboratory, USA, 2015
73. F. Cérou, A. Guyader, Adaptive multilevel splitting for rare event analysis, Stoch. Anal. Appl. **25**, 417 (2007)
74. C.E. Bréhier et al., Unbiasedness of some generalized adaptive multilevel splitting algorithms, Ann. Appl. Prob. **26**, 3559 (2016)
75. H. Louvin et al., Adaptive multilevel splitting for Monte Carlo particle transport, EPJ Web Conf. **153**, 06006 (2017)
76. H. Louvin et al., Adaptive multilevel splitting for Monte Carlo particle transport, EPJ Nuclear Sci. Technol. **3**, 29 (2017)
77. H. Louvin, E. Dumonteil, T. Lelièvre, Three-dimensional neutron streaming calculations using adaptive multilevel splitting, in *Proc. M&C2017, Jeju, Korea*, (2017)
78. H. Louvin, O. Petit, Application of adaptive multilevel splitting on coupled neutron-photon TRIPOLI-4 Monte Carlo simulations, in *Proc. RPSD2018, Santa Fe, USA*, (2018)
79. Y.K. Lee, 14 MeV neutron streaming calculations for JET-like maze entrance using TRIPOLI-4 Monte Carlo code, Fusion Eng. Design **146**, 2163 (2019)
80. J.C. Jaboulay et al., Rigorous-two-Steps scheme of TRIPOLI-4 Monte Carlo code validation for shutdown dose rate calculation, EPJ Web Conf. **153**, 02008 (2017)
81. J.A. Kulesza et al., MCNP Code Version 6.3.0 Theory & User Manual, Technical Report LA-UR-22-30006, Los Alamos National Laboratory, USA, 2022
82. P. Ridoux et al., Improvement of gamma-ray Sn transport calculations including coherent and incoherent scatterings and secondary sources of bremsstrahlung and fluorescence: Determination of gamma-ray buildup factors, Nucl. Sci. Eng. **123**, 215 (1996)
83. D. Riz, Calculation and use of multigroup cross sections including electron-photon cascade for a 3D Monte Carlo neutron-gamma transport code. Comparisons with MCNP-4B, in *Proc. Physor2000, Pittsburgh, USA*, (2000)
84. D. Mancusi, A. Bonin, F.X. Hugot, F. Malouch, Advances in Monte-Carlo code TRIPOLI-4's treatment of the electromagnetic cascade, EPJ Web Conf. **170**, 01008 (2018)
85. D. Mancusi, A. Bonin, F.X. Hugot, F. Malouch, Advances in the treatment of the electromagnetic cascade in the TRIPOLI-4 Monte Carlo Code, IEEE Trans. Nucl. Sci. **65**, 2372 (2018)
86. M.J. Berger, S.M. Seltzer, Bremsstrahlung and photoneutrons from thick tungsten and tantalum targets, Phys. Rev. C **2**, 621 (1970)
87. S.M. Seltzer, M.J. Berger, Bremsstrahlung energy spectra from electrons with kinetic energy 1 keV–10 GeV incident on screened nuclei and orbital electrons of neutral atoms with Z = 1–100, Atom. Data Nucl. Data **35**, 345 (1986)
88. S. Goudsmit, J.L. Saunderson, Multiple scattering of electrons, Phys. Rev. **57**, 24 (1940)
89. S.T. Perkins, D.E. Cullen, S.M. Seltzer, Tables and graphs of electron-interaction cross sections from 10 eV to 100 GeV derived from the LLNL Evaluated Electron Data Library (EEDL), Z = 1–100, Tech. Rep. UCRL50400, Lawrence Livermore National Laboratory, 1991
90. N.F. Mott, The scattering of fast electrons by atomic nuclei, Proc. Roy. Soc. Ac. **124**, 425 (1929)
91. G. Molière, Theorie der Streuung schneller geladener Teilchen i: Einzelstreuung am abgeschirmten CoulombFeld, Z. Naturforsch. **2**, 133 (1947)
92. G. Molière, Theorie der Streuung schneller geladener Teilchen ii: Mehrfach- und Vielfachstreuung, Z. Naturforsch. **3**, 78 (1948)
93. H. Feshbach, The Coulomb scattering of relativistic electrons and positrons by nuclei, Phys. Rev. **88**, 295 (1952)
94. N. Sherman, Coulomb scattering of relativistic electrons by point nuclei, Phys. Rev. **103**, 1601 (1956)
95. D.A. Brown et al., ENDF/B-VIII.0: The 8th Major Release of the Nuclear Reaction Data Library with CIELO-project Cross Sections, New Standards and Thermal Scattering Data, Nucl. Data Sheets **148**, 1 (2018)
96. O. Iwamoto et al., Japanese evaluated nuclear data library version 5: JENDL-5, J. Nucl. Sci. Technol. **60**, 1 (2023)
97. T.K. Tuyet, A. Jinaphanh, C. Jouanne, F. Gérardin, S. Lemaire, A. Zoia, Comparison of the TRIPOLI-4, DIANE, and MCNP6 Monte Carlo Codes on the Barber & George Benchmark for Photonuclear Reactions, Nucl. Sci. Eng. **198**, 319 (2024)
98. M. Caillaud, S. Lemaire, S. Ménard, P. Rathouit, J.C. Ribes, S. Riz, DIANE multiparticle transport code, in *Proc. SNA+MC2013, Paris, France*, (2014)
99. J. Allison et al., Recent developments in Geant4, Nucl. Instrum. Meth. Phys. Res. A **835**, 186 (2016)
100. D. Mancusi, O. Bringer, P. Monot, Progress on the TRIPOLI-4-Geant4 coupling, EPJ Web Conf. **153**, 06002 (2017)
101. J.M. Verbeke, O. Petit, O. Litaize, A. Chebboubi, Correlated production and analog transport of fission neutrons and photons using fission models FREYA, FIFRELIN and the Monte Carlo code TRIPOLI-4, IEEE Trans. Nucl. Sci. **65**, 2471 (2018)
102. O. Petit, C. Jouanne, O. Litaize, O. Serot, A. Chebboubi, Pénéliau, FIFRELIN-TRIPOLI-4 coupling for Monte

Carlo simulations with a fission model. Application to shielding calculations, EPJ Web Conf. **153**, 06003 (2017)
103. J.M. Verbeke, O. Petit, Stochastic analog neutron transport with TRIPOLI-4 and FREYA: Bayesian uncertainty quantification for neutron multiplicity counting, Nucl. Sci. Eng. **183**, 214 (2016)
104. O. Petit, E. Dumonteil, Analog neutron transport for nuclear instrumentation applications with the Monte Carlo code TRIPOLI-4, Nucl. Technol. **192**, 259 (2015)
105. J.M. Verbeke, J. Randrup, R. Vogt, Fission Reaction Event Yield Algorithm, FREYA - For event-by-event simulation of fission, Comput. Phys. Commun. **191**, 178 (2015)
106. O. Litaize, O. Serot, Investigation of phenomenological models for the Monte Carlo simulation of the prompt fission neutron and γ emission, Phys. Rev. C, Nucl. Phys. **82**, 054616 (2010)
107. C. Larmier, M.A. Kowalski, A. Zoia, CASTOR, a random media sampler for particle transport applications, in *Proc. M&C23, Niagara Falls, Canada*, (2023)
108. C. Larmier, E. Dumonteil, F. Malvagi, A. Mazzolo, A. Zoia, Finite-size effects and percolation properties of Poisson geometries, Phys. Rev. E **94**, 012130 (2017)
109. C. Larmier, A. Zoia, F. Malvagi, E. Dumonteil, A. Mazzolo, Monte Carlo particle transport in random media: The effects of mixing statistics, J. Quant. Spectr. Radiat. Transfer **196**, 270 (2017)
110. G.C. Pomraning, *Linear Kinetic Theory and Particle Transport in Stochastic Mixtures* (World Scientific Publishing, River Edge, USA, 1991)
111. S. Torquato, *Random Heterogeneous Materials: Microstructure and Macroscopic Properties* (Springer-Verlag, New York, USA, 2013)
112. C. Larmier, A. Zoia, F. Malvagi, E. Dumonteil, A. Mazzolo, Neutron multiplication in random media: Reactivity and kinetics parameters, Ann. Nucl. Energy **111**, 391 (2018)
113. C. Larmier, F.X. Hugot, F. Malvagi, A. Mazzolo, A. Zoia, Benchmark solutions for transport in d-dimensional Markov binary mixtures, J. Quant. Spectr. Radiat. Transfer **189**, 133 (2017)
114. A. Marinosci, C. Larmier, A. Zoia, Neutron transport in anisotropic random media, Ann. Nucl. Energy **118**, 406 (2018)
115. H. Belanger, C. Larmier, D. Mancusi, A. Zoia, Optimization of Particle Tracking Methods for Stochastic Media, in *Proc. of Physor2022, Pittsburgh, USA*, 2022
116. C. Larmier, A. Lam, P. Brantley, F. Malvagi, T. Palmer, A. Zoia, Monte Carlo chord length sampling for d-dimensional Markov binary mixtures, J. Quant. Spectr. Radiat. Transfer **204**, 256 (2018)
117. C. Larmier, A. Zoia, F. Malvagi, E. Dumonteil, A. Mazzolo, Poisson-Box Sampling algorithms for three-dimensional Markov binary mixtures, J. Quant. Spectr. Radiat. Transfer **206**, 70 (2018)
118. Y.K. Lee, Organ dose calculations using ICRP adult voxel phantoms and TRIPOLI-4 Monte Carlo code, ASME J. Nucl. Rad. Sci. **6**, 041105 (2020)
119. Y.K. Lee, F.X. Hugot, Y. Jin, New route in TRIPOLI-4 for radiation dosimetry calculations using ICRP 110 voxel phantoms, in *Proc. of M&C 2021, Raleigh, USA*, (2021)
120. Y.K. Lee, F.X. Hugot, Current status of TRIPOLI-4 Monte Carlo radiation transport code on adult and pediatric computational phantoms for radiation dosimetry study, Nucl. Sci. Eng. **198**, 274 (2024)
121. L. Struelens et al., Joint EURADOS-EANM initiative for an advanced computational framework for the assessment of external dose rates from nuclear medicine patients, EJNMMI Phys. **11**, 38 (2024)
122. J. Wagner, D.E. Peplow, S.W. Mosher, FW-CADIS method for global and regional variance reduction of Monte Carlo radiation transport calculations, Nucl. Sci. Eng. **176**, 37 (2014)
123. M.A. Kowalski, L. Larmier, F. Madiot, J. Durand, S. Lemaire, A. Zoia, Particle transport in Markov media with spatial gradients: Comparison between reference solutions and Chord Length Sampling, J. Quant. Spectr. Radiat. Transfer **286**, 108185 (2022)
124. A. Jinaphanh, A. Zoia, A variance-reduction strategy for the sensitivity of β_{eff}, in *Proc. of SNA+MC2024, Paris, France*, (2024)
125. C. Montecchio, D. Mancusi, A. Zoia, Towards a highly efficient and unbiased population-control algorithm for kinetic Monte Carlo simulations, in *Proc. of SNA+MC2024, Paris, France*, (2024)
126. P. Vinai et al., On the simulation of neutron noise induced by vibrations of fuel pins in a fuel assembly, Ann. Nucl. Energy **181**, 109521 (2023)
127. M. Hursin et al., Modeling noise experiments performed at AKR-2 and CROCUS zero-power reactors, Ann. Nucl. Energy **194**, 110066 (2023)
128. H. Belanger, D. Mancusi, A. Rouchon, A. Zoia, Variance reduction and noise source sampling techniques for Monte Carlo simulations of neutron noise induced by mechanical vibrations, Nucl. Sci. Eng. **197**, 534 (2023)

Cite this article as: François-Xavier Hugot, Alexis Jinaphanh, Cédric Jouanne, Coline Larmier, Yi Kang Lee, Davide Mancusi, Odile Petit, Thierry Visonneau, Andrea Zoia. Overview of the TRIPOLI-4 Monte Carlo code, version 12, EPJ Nuclear Sci. Technol. **10**, 17 (2024)